Plasma Sources
Science and
Technology

PAPER • **OPEN ACCESS**

Controlling: the composition of plasma-activated water by Cu ions

To cite this article: Kinga Kutasi *et al* 2021 *Plasma Sources Sci. Technol.* **30** 045015

OPEN ACCESS
IOP Publishing
Plasma Sources Science and Technology
Plasma Sources Sci. Technol. **30** (2021) 045015 (11pp)
https://doi.org/10.1088/1361-6595/abf078

Controlling: the composition of plasma-activated water by Cu ions

Kinga Kutasi[1,*], Nikša Krstulović[2], Andrea Jurov[3], Krešimir Salamon[4], Dean Popović[2] and Slobodan Milošević[2]

[1] Wigner Research Centre for Physics, POB 49, H-1525 Budapest, Hungary
[2] Institute of Physics, Bijenička cesta 46, 10000 Zagreb, Croatia
[3] Jožef Stefan International Postgraduate School, Jamova 39, Ljubljana 1000, Slovenia
[4] Ruđer Bošković Institute, Bijenička cesta 54, 10000 Zagreb, Croatia

E-mail: kutasi.kinga@wigner.mta.hu

Received 11 December 2019, revised 10 February 2021
Accepted for publication 19 March 2021
Published 27 April 2021

Abstract

It is demonstrated that Cu ions can be used to control the ageing of plasma-activated liquids through the Fenton-type reaction, which acts as a competitor to the $NO_2^- + H_2O_2 + H^+ \rightarrow$ *products* reaction, and thus moderates the recombination of NO_2^- ions. It is shown that the ageing dynamics is influenced by the type of Cu-ions source used, due to the different ion dissolution dynamics. Using CuNP-colloidal and copper acetate salt solutions, respectively, similar ageing dynamics can be achieved: the lifetime of NO_2^- can be increased to 10^4 min comparing to 10^2 min obtained in plasma-activated water, while the H_2O_2 concentration decreases to about half of its initial value. While the treated salt solutions contain the degradation products of the salt compounds, the CuNPs can be filtered out from the plasma-activated colloid (PAC). It is shown that filtration does not influence the concentration of active species, while the ageing of the filtrated PAC depends on the moment of filtration, which determines the concentration of dissolved Cu ions. Using copper foil, the dissolved Cu-ion concentration can be controlled by removing the foil during ageing, and in this way the lifetime of species and the H_2O_2 concentration can be adjusted. The effect has been validated in the case of two different plasma sources: a surface-wave microwave discharge and a kHz plasma jet, which produce PALs with different $[NO_2^-]/[H_2O_2]$ concentration ratio, which is the main governor of the ageing process.

Keywords: plasma-activated colloid, plasma-activated liquid, surface-wave microwave discharge, plasma jet, laser ablation in liquids

(Some figures may appear in colour only in the online journal)

1. Introduction

In the last decade plasma-activated liquid (PAL) has received a lot of attention from the plasma medicine and plasma agriculture community due to its potential to induce oxidative stress to cells. The active species (mostly reactive oxygen and nitrogen species (RONS)) created by the plasma–liquid interaction in the liquid phase have been found to have antimicrobial and antibacterial effect [1–11]. In general, the results are attributed to the synergetic effect between the RONS and/or pH of the solution [3, 5]. By conducting more detailed investigations, Ikawa *et al* [12] have suggested that the bactericidal effect can be attributed to the peroxynitrous acid (ONOOH) or peroxynitric acid (O_2NOOH) stored in the plasma-activated water (PAW), which can release O_2^-. Schmidt *et al* [13] have also found that the plasma-activated tap water has stronger antibacterial effect than the plasma-activated deionized water

* Author to whom any correspondence should be addressed.

(DIW), although the pH-value of tap water does not decrease during the plasma treatment, and its conductivity increases less than for the other tested liquids. It is assumed that the increased antimicrobial effect in tap water, despite the constant pH, can be attributed to the presence of sodium bicarbonate ($NaHCO_3$) (whose effect has been already detected by Marotta *et al* [14] in the degradation of phenol in plasma-treated tap water). Sodium bicarbonate maintains the pH-value of the liquid, while being a quencher for OH radicals, but it also leads to the formation of the CO_3^- anion, which oxidizes organic compounds efficiently (its oxidation potential being 1.78 V at pH. 7.0) [15].

In the field of agriculture it has been shown that the PAW can improve the seed germination and the plant growth [16–18], and can increase the stress tolerance [19]. Recently the protection of plants against infections by PAW has also been targeted. Perez *et al* [20] have studied the PAW as resistance inducer against bacterial leaf spot of tomato caused by *X. vesicatoria* (*Xv*), which is widely spread in all the areas where tomato is cultivated, due to the lack of effective pesticides. Although the PAW has not shown direct antimicrobial activity against *Xv* in *in vitro* experiments, it enhanced the tomato plants defenses. ten Bosch *et al* [21] have tested the PAW as a pesticide, for the possible treatment of a mealybug (*P. citri*) infestation. With the PAW application high mortality rates of approx. 90% have been achieved after an observation period of 24 h, and it is concluded, that the PAW is promising for the treatment of smaller plant stock and commodities as produced by small scale farmers or in greenhouses as an environmentally friendly substitute or supplement to conventional pesticides.

In order to be able to identify the role of different species in the interaction of PALs with biological systems and to optimize the applications, it would be important to achieve the production of PALs with very different compositions by a single source and to be able to control their ageing. According to the data found in the literature [3–6, 22–34], the composition of the reported PALs and the volume to be activated depend on the plasma source. The dielectric barrier discharge activated liquids are nitrite/nitrate dominated, while with plasma jets higher H_2O_2 concentrations can be obtained. Data also show that buffered solutions result in PAL with different pH and composition than the DIW [35]. In phosphate buffered solutions lower H_2O_2 and higher nitrate/nitrite concentrations have been achieved [6, 27, 30], however contradictory results have been also reported (see table 2 in [35]). It is also well known that the composition of the PAL also changes during storage, and the total recombination of RONS can also occur. The lifetime of the PAL—followed either through the lifetime of different RONS or the PAL's activity retention time—has been found to vary from days to months, depending on the plasma source used, i.e. on its initial composition, and on the storage temperature [5, 22, 23, 36–38].

The tuning of the PAW's composition during the treatment phase has been obtained in a limited range by Ito *et al* [39] and Wang *et al* [40] by varying the gas flow rate of the shielding and discharge gas, respectively. Recently, we have shown that a surface-wave microwave discharge is suitable for tuning the PAW's composition in a wide range, and the ageing of the PAW depends on the absolute concentration of the species [41]. It has been found that the early stage ageing is controlled by the concentration of the H_2O_2, which determines first of all the recombination of NO_2^-, through the $NO_2^- + H_2O_2 + H^+ \rightarrow products$ reaction. Namely, at H_2O_2 molar concentrations higher than that of NO_2^-, the NO_2^- recombines within few hours. We have shown that the kinetics of the H_2O_2 can be controlled with the help of a Fenton-type reaction by introducing copper surface into the PAW. As a consequence, the ageing dynamics can be changed and the lifetime of NO_2^- can be increased.

The aim of the present work is to validate the effect previously achieved with a copper plate and to test the effect of the copper ions—which were found to mediate the ageing of PAW—originating from different sources: (i) copper foil, that is a bulk surface, (ii) CuNP-colloid, where the surface-area to volume ratio is larger, and (iii) copper salts.

2. Experimental methods

2.1. Copper colloidal solution

The colloidal solution is synthesized by laser ablation of Cu target (purity: 99.9%) in purified water. The experimental setup has been described in details in [42]. Accordingly, the target is immersed in a beaker containing water and kept at constant depth (2 cm) during the synthesis, in order to keep the laser-ablation efficiency constant [43]. The 1064 nm Nd:YAG laser (Brilliant, Quantell) is focussed on the target, that is ablated with 10 000 pulses in 50 ml of water. The pulse duration is 4 ns with a repetition rate of 5 Hz. The energy delivered to the target surface is 120 mJ, while the beam width on the target surface is 338 μm, which yields a laser pulse fluence of 34 J cm^{-2}. From the volume of the craters left on the surface after ablation the amount of ablated material forming the colloidal solution can be determined [44, 45]. The volume of the ablated material is found to be 20×10^6 μm^3, which corresponds to 0.51 mg of ablated materials per crater (or per 50 ml solution), which yields the mass concentration of ablated species to be 10^{-2} mg ml^{-1}.

The synthesized colloidal solutions are characterized by optical absorbance measured with the UV–Vis spectrophotometer (Lambda 25, Perkin Elmer) in the 190–800 nm wavelengths range. The morphology and the size-distribution of the CuNPs in the colloid are studied by scanning electron microscopy (SEM) images (Jeol JSM-7600F). Few drops of the CuNP-colloid are dropped onto a Si substrate, and analysed by SEM after the water evaporation. The size-distribution shows a log–normal distribution (figure 1(a)), which is typical for the NPs synthesized by laser ablation in water [45, 46], with the average CuNP diameter of 38 nm.

The SEM image (figure 1(b)) shows that additionally to the CuNPs, a certain amount of ablated material formed irregular surfaces (flakes) rather than NPs. The crystallinity and phase of the CuNPs are determined using Siemens D5000 x-ray diffractometer with Cu Kalpha-radiation and Göbel mirror in grazing incidence (GI) geometry. The GIXRD measurements are performed with the fixed incidence angle of 1°. According to the GIXRD spectrum shown in figure 1(c), the diffraction peaks

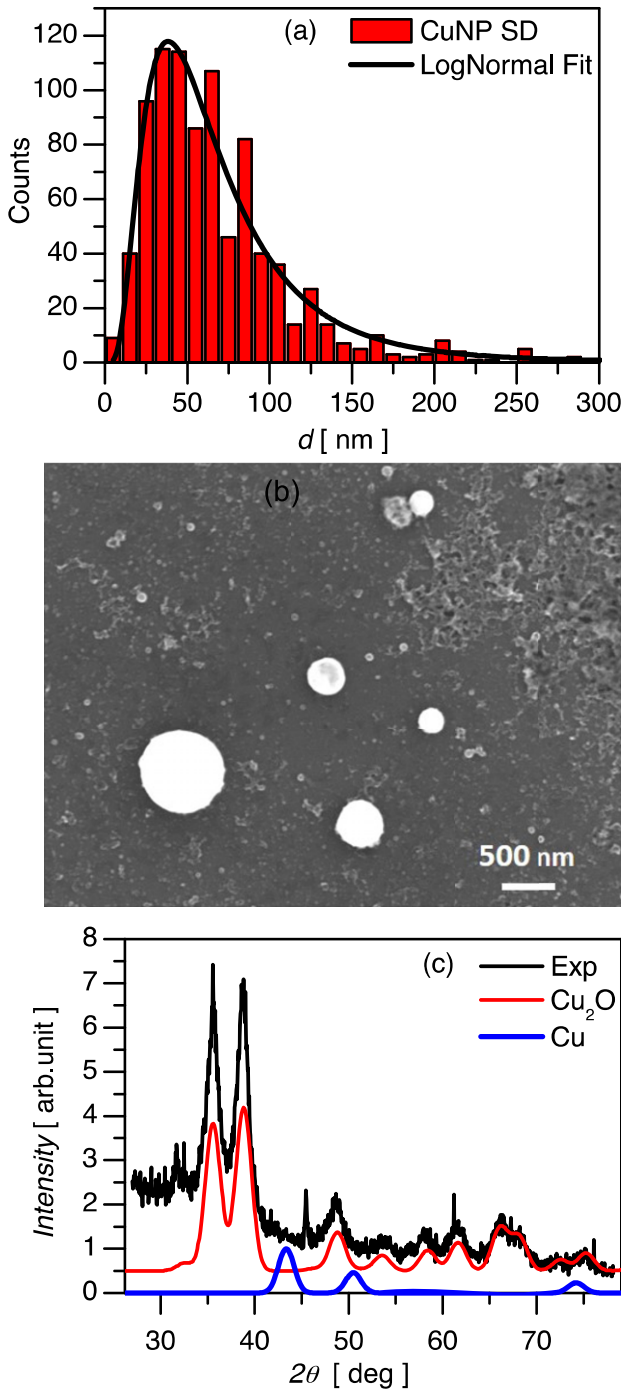

Figure 1. (a) Size distribution of the colloid particles. (b) Typical SEM image of the colloid particles deposited on Si substrate. (c) GI x-ray spectrum of the colloid particles compared to the CuNPs and Cu_2ONPs spectra.

match to the Cu_2O phase, showing that oxidized rather than pure CuNPs are formed. The zeta potential (ζ) of the Cu_2ONPs is determined by electrophoretic light scattering, using the Zetasizer Ultra (Malvern Panalytical, UK). ζ is calculated from the measured electrophoretic mobility by means of the Henry equation using the Smoluchowski approximation (f(ka) = 1.5) with the ZS Xplorer 1.20 (Malvern Panalytical). The ζ is found to be 13.7 ± 0.6 mV. In accordance to this, the colloid has been stable for several weeks.

2.2. Preparation of PAL

Active species are generated in purified water (produced with the ELGA Purelab Option-R 7 purifier), copper colloidal and salt solutions by putting the liquid surface in contact with the plasma plume of a kHz plasma jet and of a surface-wave microwave discharge, respectively.

The surface-wave microwave discharge is generated with the help of a surfatron launcher (Sairem, Surfatron 80) in a quartz tube of outer diameter 7 mm and inner diameter 4 mm, using Ar gas at 2000 sccm flow rate and MW input power of 25 W. A Berzelius beaker of 35 ml filled with 32 ml of liquid is positioned below the plasma plume with the liquid surface being at distance d (for each sample specified in section 3) from the edge of the quartz tube [41]. In order to avoid the overheating of the quartz tube during treatments, compressed air is applied along the quartz tube with a gas flow rate of 8 slm.

The atmospheric pressure plasma jet consists of a quartz tube with the outer and inner diameters of 1.5 and 1 mm, respectively, and a copper wire of 100 μm diameter, which is inserted in the capillary and serves as an electrode [47]. The electrode is powered with a sinusoidal voltage waveform of 28 kHz with 12 kV maximum voltage, chosen based on our previous optimization work conducted on the single electrode atmospheric pressure plasma jet [48]. The discharge is generated in N_2 (99.996% purity), which is supplied to the capillary with 500 sccm flow rate. The 25 ml sample in the Berzelius beaker is brought in contact with the plasma jet by placing the liquid surface at 5 mm distance from the capillary orifice, which insures the comparable production of H_2O_2 and NO_2^- in the PAL [41].

The plasma-activated samples are analysed immediately after the treatment, as well as several times during their storage. The concentration of NO_2^-, NO_3^- and H_2O_2, and the pH of samples are measured with QUANTOFIX® test strips (Nitrate/nitrite 500, 10–500 mg l^{-1} NO_3^-, 1–80 mg l^{-1} NO_2^-; Nitrate/nitrite 100, 5–100 mg l^{-1} NO_3^-, 0.5–50 mg l^{-1} NO_2^-; Peroxide 25, 0.5–25 mg l^{-1}; Peroxide 100, 0.5–25 mg l^{-1}). The strips are evaluated with the QUANTOFIX® Relax unit (by Macherey-Nagel, GmbH), which allows quantitative analysis with high accuracy. The Nitrate/nitrite strips have been calibrated using $NaNO_2$ and $Ca(NO_3)_2$ solutions of known concentrations, and the calibration has been verified with UV–VIS absorption spectroscopy measurements. Using strips makes possible to follow the ageing of samples with 1 min time resolution without any significant consumption of the sample (i.e. the sample volume can be kept quasi-constant during ageing). The measuring error has been determined to be less than 10% [41].

3. Results and discussion

3.1. Copper ions originating from copper surfaces

First of all, the effect of a bulk copper surface is validated by using a copper foil. During the treatment the inner wall of the Berzelius beaker is wrapped with copper foil (the size of the foil is 4.5 × 10 cm). After treatment this foil is

Table 1. Summary of the different PALs discussed in section 3.1

Identification	Preparation conditions
Samples prepared with the surface-wave MW discharge using input power 25 W, Ar flow rate 2000 sccm	
PAW1	Water treated at 8 mm distance for 5 min
PA(W + Cu)1	Water with Cu foil treated at 8 mm distance for 5 min
PA(W + Cu)1-Cu	PA(W + Cu)1 with the Cu foil removed at 60 min of storage
PAC1	CuNP-colloid treated at 8 mm distance for 5 min
PAW1+W	16 ml of PAW1 + 16 ml W
PAW1 +COL	16 ml of PAW1 + 16 ml CuNP-colloid
PAC1s	CuNP-colloid treated at 8 mm distance for 5 min with stirring applied
Samples prepared with the kHz plasma jet using 28 kHz and 12 kV, N_2flow rate 500 sccm	
PAW3	Water treated at 5 mm distance for 10 min
PA(W + Cu)3	Water with Cu foil treated at 5 mm distance for 10 min
PA(W + Cu)3-Cu	PA(W + Cu)3 with the Cu foil removed at 60 min of storage
PAC3	CuNP-colloid treated at 5 mm distance for 10 min

transferred to the storing container together with the PAW. As a control sample, a plasma-activated water (PAW1) is also produced. The samples are prepared with the Ar surface-wave microwave (MW) discharge (see section 2.2) using treatment time of 5 min, and treatment distance of 8 mm (as listed in Table 1), which according to the previous studies [41] results in PAL with relatively high H_2O_2 concentration, such as 40–50 mg l^{-1}.

The first column of figure 2 shows the composition and the pH of the two samples, as well as their evolution during storage. After the treatment, in the case of the PAW1 the NO_2^- concentration starts to decrease strongly, and as a consequence, the NO_2^- disappears totally at about 200 min of storage. This occurs due to the high H_2O_2 concentration, since as already discussed in [41], the rate of the concentration decrease depends on the absolute concentrations, most importantly on that of the H_2O_2. Meanwhile, the NO_3^- concentration slightly increases, since NO_3^- is one of the possible end products of the $NO_2^- + H_2O_2 + H^+ \rightarrow products$ reaction. Due to this reaction, the H_2O_2 concentration also decreases during the first 100 min, after which stabilizes at about half of its initial value. When applying the copper foil (PA(W + Cu)1 sample), contrary to the PAW1 case, the H_2O_2 concentration does not stabilize after 100 min of storage, but decreases further with an even higher rate, and as a consequence, H_2O_2 disappears on the 2nd day (at 2000 min) of storage. On the other hand, the nitrite concentration stays quasi-stable up to one week (10^4 min). The pH of the liquid shows a strong correlation with the H_2O_2 concentration, i.e. the pH increases monotonically with the decrease of the H_2O_2 concentration. Although the initial pH of the PAW1 and PA(W + Cu)1 are both close to 5.5, their ageing is different. While the pH of the PA(W + Cu)1 increases to 6 during one week of storage, the pH of the PAW1 decreases to 4.5.

The effect of the copper foil is attributed to the copper ions participating in the Fenton-type reaction (similar effect is applied for OH production aimed for Tungsten removal in [52]), which is believed to have more pathways: (i) the Fenton $Cu^+/Cu^{2+} + H_2O_2 \rightarrow Cu^{2+}/Cu^{3+} + OH + OH^-$ or (ii) the catalase $Cu^{2+} + H_2O_2 \rightarrow CuO^{2+} + H_2O$, $CuO^{2+} + H_2O_2 \rightarrow Cu^{2+} + H_2O + O_2$. In the case of acidic conditions the OH^- produced in the Fenton reaction can react with the H^+, i.e. $OH^- + H^+ \rightarrow H_2O$, which results in the increase of pH.

The Fenton-type reaction can occur on the surface of the copper foil or in the liquid phase due to the dissolved copper ions. Removing the copper foil the surface effect can be eliminated. By removing the copper foil (PA(W + Cu)1-Cu sample) before the second phase of H_2O_2 concentration decrease, the slowing of this phase is achieved, while the nitrite concentration decrease enhances, as shown in the first column of figure 2. As a consequence, after one week (10^4 min) of storage both the nitrite and the H_2O_2 are still present in the plasma-activated liquid. By removing the copper foil, the dissolution of Cu-ion is also stopped. The concentration of dissolved Cu-ion after one week of storage in the PA(W + Cu)1 is measured to be above 30 mg l^{-1}, while in the PA(W + Cu)1-Cu it is around 30 mg l^{-1}. From the evolution of the species concentrations for the three cases presented in the first column of figure 2, it can be concluded that, with the presence of the Cu-ions in the system, there is a competition between the Fenton-type reaction and the $NO_2^- + H_2O_2 + H^+ \rightarrow products$ reaction controlled by the active species concentrations[5].

The effect of the Cu ions originating from CuNPs is tested by using CuNP-colloidal solution in two different ways: (i) by treating directly the CuNP-colloid, i.e. creating PAC and (ii) by adding the colloidal solution (COL) to the PAW.

In the first case, the colloid is directly treated with the plasma plume under the same conditions as in the previous experiment. Comparing to the plasma-activated water, PAW1, the obtained PAC1 has a similar composition, however a slight enhancement in the species production can be observed. At the same time, during ageing, the species concentrations in

[5] Through the $NO_2^- + H_2O_2 + H^+ \rightarrow ONOOH + H_2O$ reaction peroxynitrous acid is formed, whose lifetime under acidic conditions is short and rapidly decays by homolysis $ONOOH \rightarrow NO_2 + OH$, and by izomerization $ONOOH \rightarrow NO_3^- + H^+$ to nitric acid. Peroxynitrous acid can be stabilized in basic medium $ONOOH \rightarrow ONOO^- + H^+$, pH > 6.8. During ageing it has been suggested the formation of peroxynitric acid according to $ONOOH \rightarrow O_2NOOH + H_2O$, which under acidic conditions can further homolyse according to $O_2NOOH \rightarrow NO_2 + HO_2$. On the other hand, at neutral conditions the disproportionation of peroxynitrous acid can occur: $ONOOH + ONOO^- \rightarrow NO_2^- + O_2NOO^- + H^+$, $O_2NOO^- \rightarrow NO_2^- + O_2$ [35].

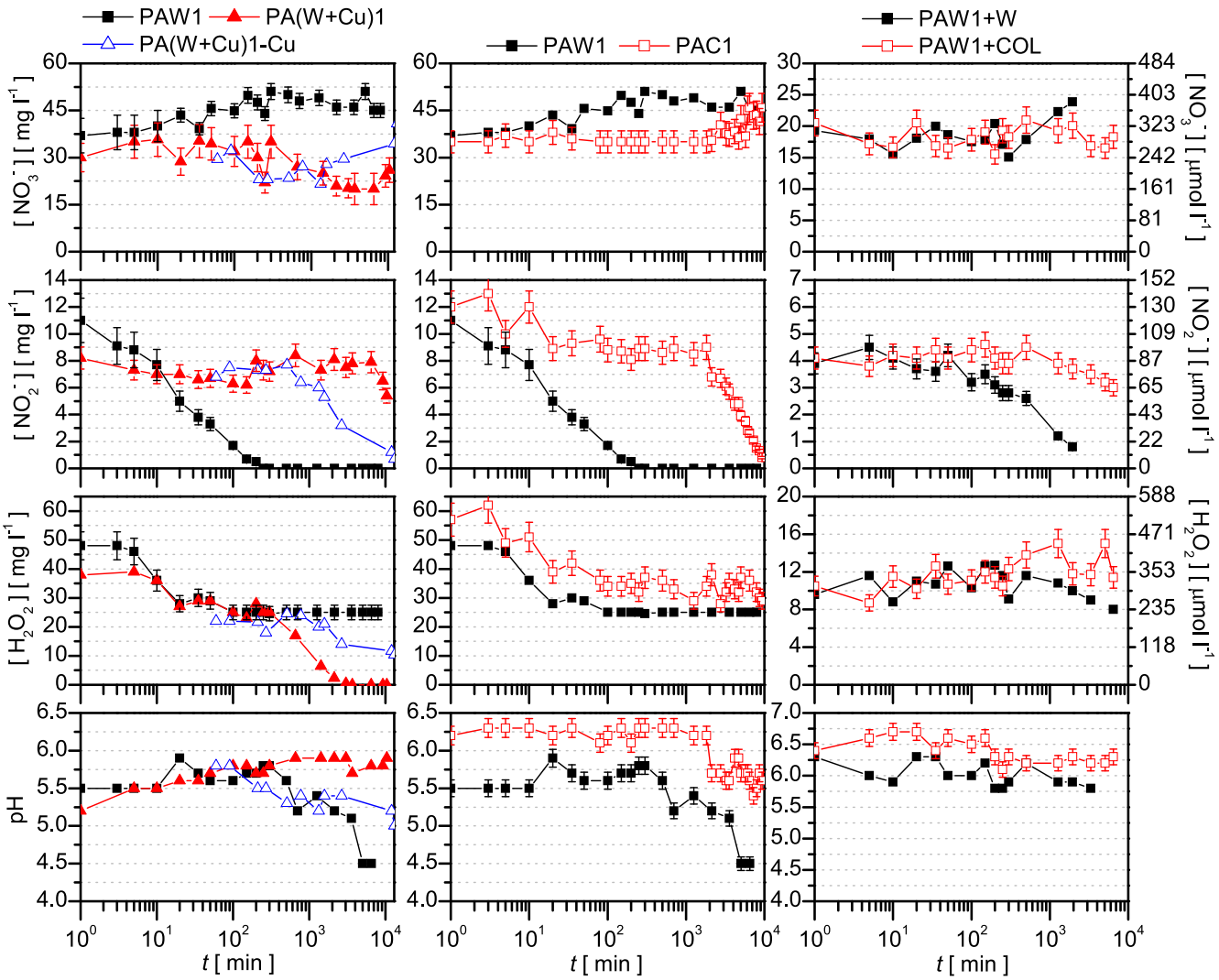

Figure 2. Ageing of the different PALs produced with the surface-wave microwave discharge as summarized in table 1, and presented as follows: the PAW and copper enriched water (first column), the plasma-activated copper colloid (second column), and the PAW diluted with water and copper colloid, respectively (third column).

the PAC exhibit different behaviour than in the PAW1, as shown in the second column of figure 2. In the case of the PAC1, the NO_2^- concentration, after a slight decrease occurring during the first 10 min, remains stable for about 2 days (2000 min). Following this, the NO_2^- concentration starts to decrease, and finally NO_2^- disappears on the 7th day (10^4 min) of storage. Meanwhile, the NO_3^- concentration slightly increases and reaches the same value as in the case of the PAW1. The H_2O_2 concentration exhibits a similar behaviour as in the case of the PAW1, i.e. decreases during the first 100 min and quasi-stabilizes at about half of its initial value. The difference between the PAW1 and PAC1 lies also in the pH of the liquids, the PAW being more acidic, 5.5 versus 6.2. The pH of the PAW1 is quasi-stable up to 400 min, after which it monotonically decreases and reaches pH 4.5 at the 7th day (10^4 min) of storage. In the case of the colloid, the acidification starts with the decrease of the nitrite concentration. After one week of storage the pH of the PAC1 reaches the initial pH of the PAW1.

Comparing the colloid and copper foil cases, although the copper ions that mediate the H_2O_2 reaction pathway are present in both liquids, the evolution of the species concentrations during storage is different. While in the case of the PA(W + Cu)1 the H_2O_2 concentration monotonically decreases to zero, in the PAC1 the H_2O_2 concentration stabilizes after 100 min, as in the case of the PAW1. As a consequence, the nitrite concentration in the PA(W + Cu)1 is quasi-stable during one week (being stable even up to 45 days at $[NO_2^-] = 5.6$ mg l^{-1}) and the nitrate concentration slightly decreases to $[NO_3^-] = 30$ mg l^{-1}. On the other hand, in the case of the PAC1 the nitrate and nitrite concentrations reach the same values as in the PAW1 with a one week delay. In the two cases the dissolved Cu-ion concentrations are found to be different. In the initial colloid the measured concentration is about 10 mg l^{-1}, which increases with plasma treatment and peaks at around 30 mg l^{-1} after few hundred minutes, while in the case of copper foil the Cu-ion concentration peaks above 30 mg l^{-1}.

For the second colloid test case, the non-treated colloid is added to the PAW1. Two different mixtures of 32 ml are created, as follows: (i) the PAW1+COL with 16 ml PAW1 and 16 ml COL, and (ii) the PAW1 + W with 16 ml PAW1 and 16 ml W, which serves as a control sample. Due to the lower species concentrations obtained through dilution, and most importantly that of the H_2O_2, the ageing dynamics also changes [41], as shown in the third column of figure 2. In both mixtures the concentrations decrease at a lower rate comparing to the PAC1 and the PAW1, respectively. As a consequence in the PAW1 + W the NO_2^- can survive 24 h longer than in the PAW1, while the H_2O_2 concentration is about half of the one obtained in the PAW1. In the PAW1 + COL sample the nitrite concentration decreases slightly during 6 days (8600 min) of storage and reaches a higher value than in the case of the PAC1, while the H_2O_2 and the nitrate concentrations are about half of the concentrations achieved in the PAC1. The more moderate concentration changes in the PAW1 + COL can also be attributed to the lower 10 mg l^{-1} Cu-ion concentration.

Comparing to the PAW and the PAC, in the diluted samples no first phase concentration decrease is observed. This may be explained with the fact that by dilution the temperature of the sample decreases fast, while the undiluted samples cool down slower to room temperature from the 40° C that are reached with the plasma treatment. As a consequence, in the case of the PAW1, PAC1 or PA(W + Cu)1, during the first 10–20 min the reaction rates are higher due to the elevated temperature.

When the role of the NPs in the plasma-activated liquid is considered to be only the control of the ageing process, and the liquid is meant to be used without NPs, it can be filtrated. The effect of filtration is tested on a plasma-activated colloid, PAC1s, produced under the same treatment conditions as PAC1. Additionally, during treatment magnetic stirring is also applied to the colloid, due to which the disturbance of the surface occurs and results in the increase of the treatment distance. As a consequence, the concentration of species in the PAC1s are lower than in the PAC1, thus the ageing dynamics is different (as previously shown in [41]).

Using a syringe filter housing 0.2 μm pore membrane, 10 ml of colloid is filtrated at 1 min and at 10455 min, respectively. Figure 3 shows the evolution of the species concentrations and the pH of the original and the filtrated colloids.

The original PAC1s is quasi-stable during the first week of storage, the concentrations decrease considerably only after 10^4 min. Nevertheless, in the following 3 days (4000 min), the nitrite and H_2O_2 concentrations decrease only by 25%. The colloid filtrated at 10^4 min follows the behaviour of the original colloid, except for the pH, which slightly decreases. On the other hand, the colloid filtrated at 1 min of storage is quasi-stable only up to 10^3 min, and the NO_2^- disappears at about 10^4 min of storage. The Cu-ion concentration measured in the colloid filtrated at 1 min of storage is 10 mg l^{-1}, while in the PAC1s it is around 30 mg l^{-1}. Overall, the filtration does not influence the concentration of active species, the filtrated colloids follow the behaviour of the original colloid for a reasonable time, which allows their usage.

The effects achieved in the liquids treated with the surface-wave microwave discharge are also validated in the case of

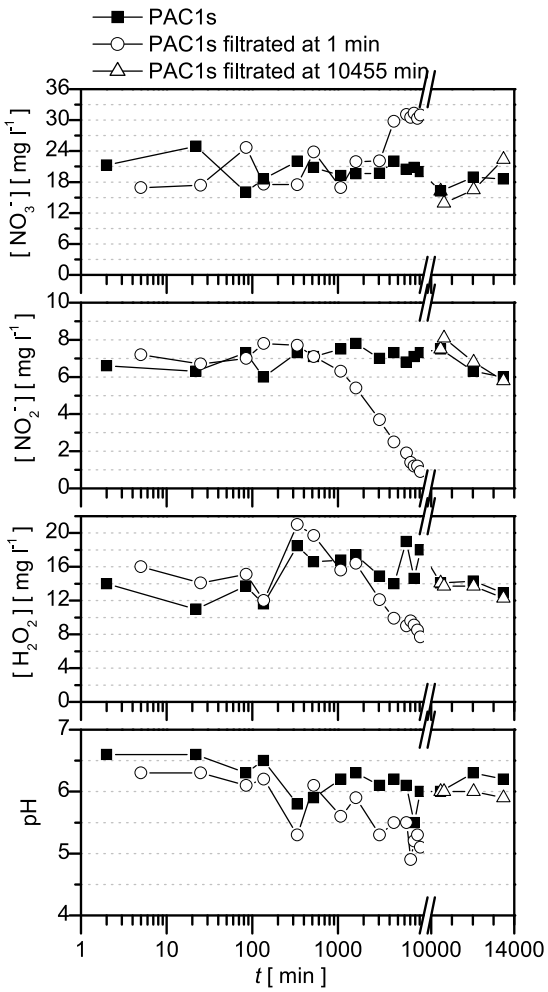

Figure 3. Ageing of the plasma-activated colloid (PAC1s) created with the MW discharge as described in table 1), and of the same colloid filtrated at 1 min and 10455 min, respectively.

a nitrogen kHz plasma jet (section 2.2), which generally, comparing to the surface-wave microwave discharge, produces lower H_2O_2 concentrations and $[H_2O_2]/[NO_2^-]$ in the PALs [41], and also results in lower PAL temperature of 30° C. Figure 4 shows the composition of the different PALs created with the plasma jet, and their evolution during storage. The molar concentration of the H_2O_2 and NO_2^- in these PAL are quasi-equal, with the H_2O_2 concentration being slightly higher. As a consequence, due to the $NO_2^- + H_2O_2 + H^+ \rightarrow$ *products* reaction, the two concentrations change similarly over time during storage. This is well illustrated by the plasma-activated water (PAW3) shown in the first column of figure 4. Due to to the slightly higher initial H_2O_2 concentration, the NO_2^- recombines totally, while the H_2O_2 is still present in the liquid after 10^4 min of storage. Contrary to the PAW3, in the case of the plasma-activated colloid (PAC3) (shown in the second column of figure 4), after 200 min the Fenton-type reaction becomes dominant over the above mentioned reaction, which results in the NO_2^- concentration to decrease at a lower rate. As a consequence, after 10^4 min both the NO_2^- and H_2O_2 are still present in the PAC3, and their concentrations are similar. Overall, the NO_3^- concentration follows the same trend as

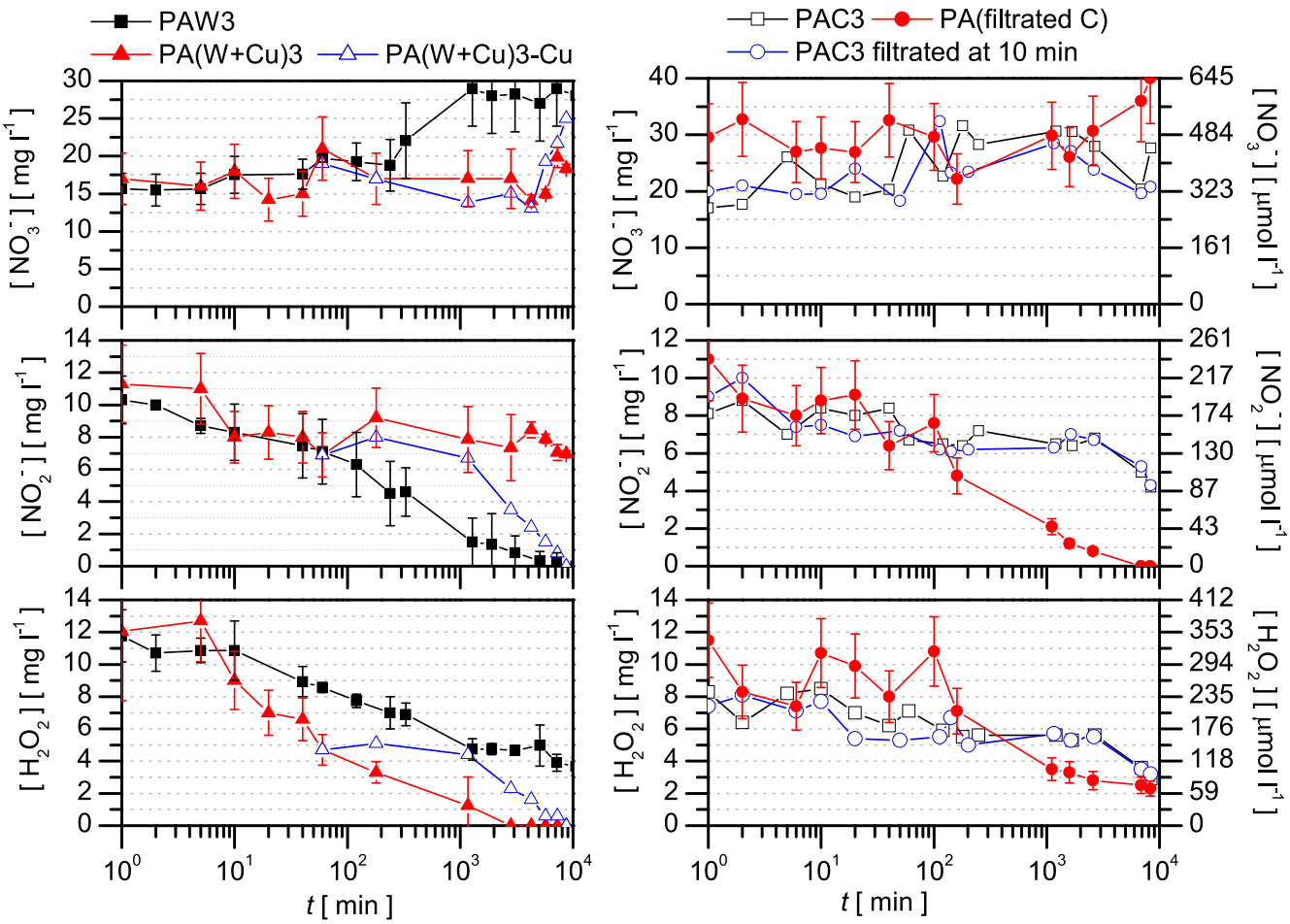

Figure 4. Ageing of the different PALs produced with the nitrogen kHz plasma jet as summarized in table 1, and presented as follows: the PAW and copper enriched water (first column), the plasma-activated copper colloid and filtrated colloid (second column).

in the case of the surface-wave microwave discharge activated water and colloid, respectively.

When using copper foil instead of NPs, the concentration of species show very similar behaviour during ageing (first column of figure 4), however, in the case of the H_2O_2 concentration the decreasing rate is faster. Comparing to the MW sample, although the initial H_2O_2 concentration in the PA(W + Cu)3 is about 3 times lower than in the case of MW discharge activated sample, the H_2O_2 disappears from the liquid on the same timescale. Due to the lower concentrations, in order to preserve H_2O_2 in this case the copper foil should be removed earlier than in the case of MW sample. Concerning the removal of the NPs, the PAC3 filtrated at 10 min of storage shows very similar ageing dynamics as the non-filtrated PAC3. The efficiency of nanoparticle filtration is tested by treating a filtrated colloid. The species concentrations in the plasma-activated filtrated colloid (PA(filtratedC)) follow the same trend during storage as in the PAW3 (shown in figure 4), which indicates the efficiency of the filtration. This is also confirmed by the UV–VIS absorption spectra shown in figure 5, where the two spectra overlap each other.

Figure 5 further shows the absorption spectra of the CuNP-colloid, the plasma-activated colloid (PAC3) and PAW3 produced with the N_2 plasma jet and measured after 10 min

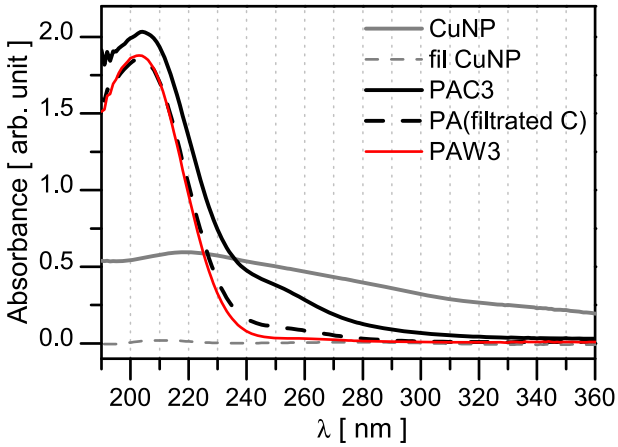

Figure 5. Absorption spectra of the CuNP-colloid, the PAC and PAW produced with the N_2 plasma jet.

of storage. The UV–Vis spectrum of the CuNP-colloid shows transparency in the visible (not shown here), and high absorbance in the UV part of spectrum, exhibiting a weak shoulder at 330 nm (blue-shifted from visible, typical peak of pure Cu nanoparticles (NPs) occurs at around 600 nm [49]), which is a typical spectrum for the Cu-oxide NPs. It

Table 2. Summary of the different PALs discussed in section 3.2

Identification	Preparation conditions
Samples prepared with the surface-wave MW discharge using input power 25 W, Ar flow rate 2000 sccm	
PAW1	Water treated at 8 mm distance for 5 min
PAC1	CuNP-colloid treated at 8 mm distance for 5 min
PA(CuAC)1	0.5 mM copper acetate solution treated at 8 mm distance for 5 min
PAC2	CuNP-colloid treated at 9 mm distance for 5 min
PA(CuAC)2	0.5 mM copper acetate solution treated at 9 mm distance for 5 min
PA($CuCl_2$)	0.5 mM copper chloride solution treated at 8 mm distance for 5 min
Samples prepared with the kHz plasma jet using 28 kHz and 12 kV, N_2 flow rate 500 sccm	
PAC3	CuNP-colloid treated at 5 mm distance for 10 min
PA(CuAC)3	0.5 mM copper acetate solution treated at 5 mm distance for 10 min

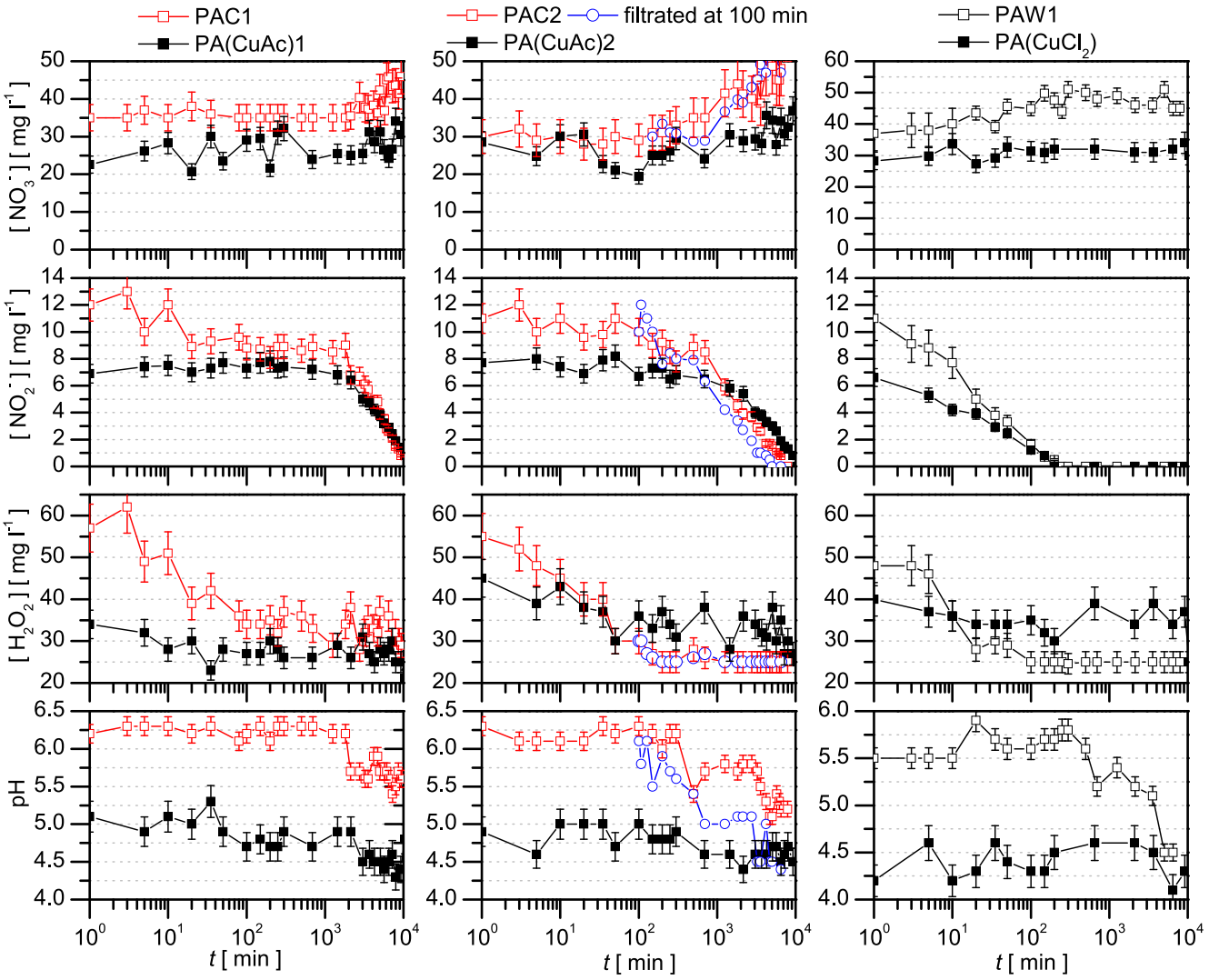

Figure 6. Ageing of the plasma-activated CuNP-colloids and copper salt solutions produced with the surface-wave microwave discharge as described in Table 2.

is known that the ablated Cu oxidizes due to the interaction with dissolved oxygen in water [50]. The absorption spectra of the filtrated colloid indicates a very efficient filtration, as no significant absorption is observed in the relevant spectral range. During plasma treatment one observes the colour change of the colloidal solution (from greenish to transparent), which indicates the agglomeration of NPs. The change of the colloid is also illustrated by the UV absorption spectra, showing the decrease of the absorbance above 225 nm. Meanwhile, due to the creation of different species by the plasma

treatment, a strong absorption occurs in the 190–240 nm spectral range. The UV absorption in the plasma-activated waters has been analysed in details by Oh *et al* [51], and the absorption in the 190–240 nm spectral range has been attributed to the absorption of the dissolved O_2, and the created H_2O_2, NO_2^- and NO_3^- species. In the present samples there is no significant dissolved O_2 (since Ar and N2 discharges have been used), thus the absorption can be attributed to the created H_2O_2, NO_2^- and NO_3^- species.

3.2. Copper ions originating from copper salts

The effect of the Cu ions originating from salts is tested by using 0.5 mM copper acetate ($Cu(CH_3COO)_2$) and copper chloride ($CuCl_2$) solutions. The composition of the salt solutions treated with the Ar surface-wave microwave discharge at the same conditions as the colloidal solutions (as listed in table 2) are shown in figure 6, in comparison with that of the plasma-activated CuNP-colloids and PAW, respectively. The first salt sample is a plasma-activated copper acetate solution, PA(CuAc)1, created under the same conditions as the PAC1. One obvious difference between the two samples, as shown in the first column of figure 6, is the higher species concentrations obtained in the PAC. The salt solutions are prepared with a copper ion concentration of 32 mg l^{-1}, which in the PAC is measured after 200 min ageing, while in the initial CuNP-colloid the Cu-ion concentration is about 10 mg l^{-1}. The higher Cu-ion concentration during plasma treatment can result in the lower H_2O_2 concentration in the treated salt solution.

The PA(CuAc)1 also exhibits a slightly different ageing dynamics. The strong first phase concentration decrease characteristic for the PACs and the PAWs during the first 100–200 min of storage, in the case of the PA(CuAc)1 is more moderate and it occurs only in the case of H_2O_2. This can be attributed to the higher Cu-ion concentration in the PA(CuAc)1 in this phase, due to which, the reaction kinetics is dominated by the Fenton-type of reaction over the reaction of H_2O_2 with nitrite ions. After the first phase, the two liquids show similar behaviour over time, and at about 5×10^3 min of storage the nitrite and H_2O_2 concentrations, respectively, become quasi-equal. Meanwhile, the nitrate concentration is about 30% higher in the PAC1. At this point the main difference between the two liquids is the pH, which is about 4.5 in the PA(CuAc)1 and 5.5 in the PAC1. The effect has also been validated on liquids treated at a higher 9 mm distance, the PA(CuAc)2 and the PAC2, as shown in the second column of figure 6 (illustrating the reproducibility of the method).

Due to the degradation products of salts and their reaction with the active species of interest, a careful choice of the salt type is needed. While with the application of the CuAc similar effects can be achieved as with the CuNP-colloid, by choosing $CuCl_2$ the concentration of active species behave differently (third column of figure 6). Although the ageing of the PA($CuCl_2$) is similar to that of the PAW1, the reaction kinetics is more complex, and additionally under acidic conditions the formation of hydrogen chloride can also be expected. By treating copper acetate solution with the plasma jet similar ageing behaviour is obtained as in the case the MW treated solution.

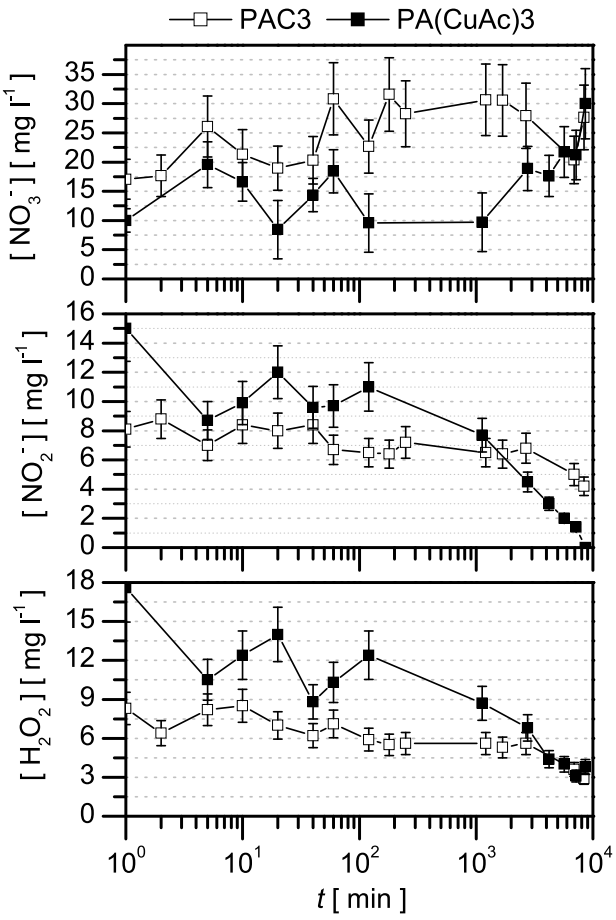

Figure 7. Ageing of the plasma-activated CuNP-colloid and copper acetate solution produced with the N_2 plasma jet as described in table 2.

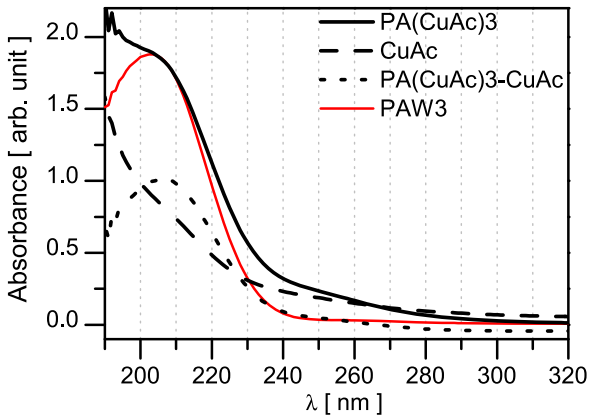

Figure 8. Absorption spectra of the plasma-activated copper acetate and the PAW produced with the N_2 plasma jet.

The evolution of the species concentrations over storage time is shown in figure 7 in comparison with the case of the treated colloid.

Overall, the CuNP-colloid and CuAc have similar effect on the PAW composition. However, while the CuNPs can be filtrated from the colloid, as proven by the UV–VIS absorption spectra shown in Figure 5, in the case of the PA(CuAc) different compounds created through plasma decomposition

of acetate are also present. Comparing the absorption spectra of the PA(CuAc) to that of the PAW, significant differences are found at spectral ranges below 210 nm and above 230 nm, see figure 8. The copper acetate solution shows a strong absorption below 240 nm. However, this contribution is much lower in the treated solution, which indicates that the acetate is decomposed during plasma treatment.

4. Conclusions

It has been demonstrated that Cu ions can be used to control the composition of PAL during ageing. The Cu ions react with the H_2O_2 through a Fenton-type reaction, which leads to the decomposition of H_2O_2. In the case of PAL this reaction can act as a competitor to the $NO_2^- + H_2O_2 + H^+ \rightarrow products$ reaction, and consequently can contribute to moderate the recombination of NO_2^- ions. The effect has been validated in the case of two different plasma sources: a surface-wave microwave discharge and a kHz plasma jet, which produce PAL with very different relative species concentrations and consequently, ageing dynamics.

By testing different copper ion sources: (i) copper surface, (ii) CuNP-colloid and (iii) copper salts, it has been shown that the ion dissolution dynamics influences the ageing dynamics of the PAL. In the case of the plasma-activated CuNP-colloid and copper acetate very similar concentration behaviours—significantly different to the case of the PAW—can be achieved. Most importantly, the lifetime of NO_2^- increases to 10^4 min comparing to the 10^2 min achieved in the PAW. In both cases, during the 10^4 min storage the NO_3^- concentrations increase slightly, while H_2O_2 concentrations decrease to about half of their initial values. The advantage of the CuNPs over the copper salts is that, while the NPs can be filtered out, in the treated salt solutions the salt compounds and their degradation products are additionally present. Furthermore, the plasma activation of the CuNP-colloids induces agglomeration of nanoparticles and sedimentation (while it does not change the oxidation state of the NPs), which results in even more efficient filtration than in the case of pure colloids. It has been shown that filtration does not influence the concentration of active species, while the ageing of filtrated PAC depends on the moment of filtration, which determines the concentration of dissolved copper ions.

In the case of the copper surface test, the beaker inner wall has been wrapped with Cu foil, which can also simulate a copper container. In the conducted experiments the size of the copper foil has been 4.5 cm × 10 cm, the volume of ablated material forming the 50 ml colloidal solution 20×10^6 μm^3, and the concentration of the salt solution 0.5 mM. Under these conditions, it has been found that the dissolved Cu-ion concentration is slightly higher in the case of the copper foil than in the two other cases, respectively, and leads to the total recombination of the H_2O_2 within 2×10^3 min. In order to control the Cu-ion concentration the copper foil can be removed during the ageing phase, and in this way the lifetime of species can also be adjusted. By removing the foil at 60 min of storage, similar NO_2^- lifetimes have been achieved as in the case of the CuNPs, while the H_2O_2 and NO_3^- concentrations are lower by a factor of 2. The ageing dynamics is further influenced by the oxidation state of the Cu-ion, which determines the reaction pathway of the Fenton-type reaction (presented in the third paragraph of section 3.1).

Due to the two competing reactions involving the H_2O_2, NO_2^- and the Cu ions, the ageing dynamics depends on the $[NO_2^-]/[H_2O_2]$ concentration ratio, and the Cu-ion concentration, which should be optimized to the composition of the PAL. Depending on the targeted application, which besides disinfection could also be the medical cancer therapy [53, 54], the type of ions that participate in the Fenton-type reaction can be chosen. The Cu-ion containing plasma-activated liquid could be used as pesticide and fungicide as an alternative for the copper sulphate used also in organic farming, since it may contain lower copper concentration, while being rich in active species.

Acknowledgments

The work has been supported by the Hungarian Science Foundation NKFIH, through project K-132158, by the Croatian Science Foundation, through projects IP-2013-11–2753 and IP-2019-02–6418.

Data availability statement

All data that support the findings of this study are included within the article (and any supplementary files).

ORCID iDs

Kinga Kutasi https://orcid.org/0000-0001-6082-1853
Nikša Krstulović https://orcid.org/0000-0001-6443-2417
Andrea Jurov https://orcid.org/0000-0003-0590-2743
Dean Popović https://orcid.org/0000-0003-3906-3482
Slobodan Milošević https://orcid.org/0000-0002-4455-7869

References

[1] Kamgang-Youbi G, Herry J-M, Bellon-Fontaine M-N, Brisset J-L, Doubla A and Naïtali M 2007 *Appl. Environ. Microbiol.* **73** 4791
[2] Kamgang-Youbi G,Herry J-M,Brisset J-L,Bellon-Fontaine M-N, Doubla A and Naïtali M 2008 *Appl. Microbiol. Biotechnol.* **81** 449
[3] Naïtali M, Kamgang-Youbi G, Herry J-M, Bellon-Fontaine M-N and Brisset J-L 2010 *Appl. Environ. Microbiol.* **76** 7662
[4] Ikawa S, Kitano K and Hamaguchi S 2010 *Plasma Process. Polym.* **7** 33
[5] Traylor M J, Pavlovich M J, Karim S, Hait P, Sakiyama Y, Clark D S and Graves D B 2011 *J. Phys. D: Appl. Phys.* **44** 472001
[6] Oehmigen K, Hähnel M, Brandenburg R, Wilke C, Weltmann K-D and von Woedtke T 2010 *Plasma Process. Polym.* **7** 250
[7] Oehmigen K, Winter J, Hähnel M, Wilke C, Brandenburg R, Weltmann K-D and von Woedtke T 2011 *Plasma Process. Polym.* **8** 904
[8] Kobayashi T, Iwata N, Oh J-S, Hahizume H, Ohta T, Takeda K, Ishikawa K, Hori M and Ito M 2017 *J. Phys. D: Appl. Phys.* **50** 155208

[9] Tasaki T, Ohshima T, Usui E, Ikawa S, Kitano K, Maeda N and Momoi Y 2017 *Dent. Mater. J.* **36** 422
[10] Machala Z, Tarabová B, Sersenová D, Janda M and Hensel K 2019 *J. Phys. D: Appl. Phys.* **52** 034002
[11] Zhou R, Zhou R, Prasad K, Fang Z, Speight R, Bazaka K and Ostrikov K 2018 *Green Chem.* **20** 5276
[12] Ikawa S, Tani A, Nakashima Y and Kitano K 2016 *J. Phys. D: Appl. Phys.* **49** 425401
[13] Schmidt M, Hahn V, Altrock B, Gerling T, Gerber I C, Weltmann K-D and von Woedtke T 2019 *Appl. Sci.* **9** 2150
[14] Marotta E, Ceriani E, Schiorlin M, Ceretta C and Paradisi C 2012 *Water Res.* **46** 6239
[15] Medinas D B, Cerchiaro G, Trindade D F and Augusto O 2007 *IUBMB Life* **59** 255
[16] Puač N, Gherardi M and Shiratani M 2017 *Plasma Process. Polym.* **15** 1700174
[17] Sivachandiran L and Khacef A 2017 *RSC Adv.* **7** 1822
[18] Thirumdas R, Kothakota A, Annapure U, Siliveru K, Blundell R, Gatt R and Valdramidis V P 2018 *Trends Food Sci. Technol.* **77** 21
[19] Gierczik K, Vukušić T, Kovács L, Székely A, Kocsy G, Szalai G, Milošević S, Kutasi K and Galiba G 2020 *Plasma Process. Polym.* **17** e1900123
[20] Perez S M, Biondi E, Laurita R, Proto M, Sarti F, Gherardi M, Bertaccini A and Colombo V 2019 *PLoS ONE* **14** e0217788
[21] ten Bosch L, Köhler R, Ortmann R, Wieneke S and Viöl W 2017 *Int. J. Environ. Res. Public Heath* **14** 1460
[22] Julák J, Scholtz V, Kotúčová S and Janoušková O 2012 *Phys. Medica* **28** 230
[23] Laurita R, Barbieri D, Gherardi M, Colombo V and Lukes P 2015 *Clin. Plasma Med.* **3** 53
[24] Lukes P, Dolezalova E, Sisrova I and Clupek M 2014 *Plasma Sources Sci. Technol.* **23** 015019
[25] Liu F *et al* 2010 *Plasma Processes Polym.* **7** 231
[26] Brisset J-L and Hnatiuc E 2012 *Plasma Chem. Plasma Process.* **32** 655
[27] Pavlovich M J, Chang H-W, Sakiyama Y, Clark D S and Graves D B 2013 *J. Phys. D: Appl. Phys.* **46** 145202
[28] Ercan U K, Wang H, Ji H, Fridman G, Brooks A D and Joshi S G 2013 *Plasma Process. Polym.* **10** 544
[29] van Gils C A J, Hofmann S, Boekema B K H L, Brandenburg R and Bruggeman P J 2013 *J. Phys. D: Appl. Phys.* **46** 175203
[30] Machala Z, Tarabova B, Hensel K, Spetlikova E, Sikurova L and Lukes P 2013 *Plasma Process. Polym.* **10** 649
[31] Girard F *et al* 2016 *RSC Adv.* **6** 78457
[32] Vlad I-E and Anghel S D 2017 *J. Electrost.* **87** 284
[33] Chen Z, Liu D, Chen C, Xu D, Liu Z, Xia W, Rong M and Kong M G 2018 *J. Phys. D: Appl. Phys.* **51** 325201
[34] Oh J-S, Szili E J, Ogawa K, Short R D, Ito M, Furuta H and Hatta A 2018 *Japan J. Appl. Phys.* **57** 0102B9
[35] Bradu C, Kutasi K, Magureanu M, Puač N and Živković S 2020 *J. Phys. D: Appl. Phys.* **53** 223001
[36] Brisset J-L and Pawlat J 2016 *Plasma Chem. Plasma Process.* **36** 355
[37] Shen J, Tian Y, Li Y, Ma R, Zhang Q, Zhang J and Fang J 2016 *Sci. Rep.* **6** 28505
[38] Julák J, Hujacová A, Scholtz V, Khun J and Holada K 2018 *Plasma Phys. Rep.* **44** 125
[39] Ito T, Uchida G, Nakajima A, Takenaka K and Setsuhara Y 2017 *Japan J. Appl. Phys.* **56** 01AC06
[40] Wang B, Liu D, Zhang Z, Li Q, Liu Z, Guo L, Wang X and Kong M G 2017 *J. Phys. D: Appl. Phys.* **50** 305202
[41] Kutasi K, Popović D, Krstulović N and Milošević S 2019 *Plasma Sources Sci. Technol.* **28** 095010
[42] Krstulović N, Umek P, Salamon K and Capan I 2017 *Mater. Res. Express* **4** 105003
[43] Krstulović N, Shannon S, Stefanuik R and Fanara C 2013 *Int. J. Adv. Manuf. Technol.* **69** 1765
[44] Krstulović N and Milošević S 2010 *Appl. Surf. Sci.* **256** 4142
[45] Krstulović N, Salamon K, Budimlija O, Kovač J, Dasović J, Umek P and Capan I 2018 *Appl. Surf. Sci.* **440** 916
[46] Schlemmer W *et al* 2018 *Materials* **11** 2412
[47] Zaplotnik R, Kregar Z, Bišćan M, Vesel A, Cvelbar U, Mozetič M and Milošević S 2014 *Europhys. Lett.* **106** 25001
[48] Zaplotnik R, Bišćan M, Kregar Z, Cvelbar U, Mozetič M and Milošević S 2015 *Spectrochimica Acta* B **103–104** 124
[49] Kazakevich P V, Simakin A V, Voronov V V and Shafeev G A 2006 *Appl. Surf. Sci.* **252** 4373
[50] Tilaki R M, Iraji Zad A and Mahdavi S M 2007 *Appl. Phys.* A **88** 415
[51] Oh J-S, Szili E J, Gaur N, Hong S-H, Furuta H, Kurita H, Mizuno A, Hatta A and Short R D 2016 *J. Phys. D: Appl. Phys.* **49** 304005
[52] Kim K, Lee K, So S, Cho S, Lee M, You K, Moon J and Song T 2018 *ECS J. Solid State Sci. Technol.* **7** P132–4
[53] Tanaka H, Mizuno M, Ishikawa K, Nakamura K, Kajiyama H, Kano H, Kikkawa F and Hori M 2011 *Plasma Med.* **1** 265
[54] Utsumi F *et al* 2013 *PLOS ONE* **8** e81576